Journal of Chemical Crystallography
https://doi.org/10.1007/s10870-020-00868-9

ORIGINAL PAPER

$Rb_2Co_{1.85}Ge_{1.15}O_6$: The First Quaternary, Noncentrosymmetric Rubidium Cobalt Germanate

Mohammad Usman[1] · Mark D. Smith[1] · Hans-Conrad zur Loye[1]

Received: 8 July 2020 / Accepted: 17 October 2020
© Springer Science+Business Media, LLC, part of Springer Nature 2020

Abstract

Deep blue, prism-shaped, X-ray diffraction quality single crystals of a new quaternary rubidium cobalt germanate, exact composition $Rb_2Co_{1.85}Ge_{1.15}O_6$, were grown by soaking a pre-reacted polycrystalline powder in a molten RbCl/RbF eutectic flux (melting point = 546 °C) at 700 °C in a silver reaction vessel. The complex was characterized by single crystal X-ray diffraction and its elemental composition was semi-quantitatively confirmed by energy dispersive spectroscopy (EDS). $Rb_2Co_{1.85}Ge_{1.15}O_6$ crystallizes in the noncentrosymmetric orthorhombic space group $C222_1$ with lattice parameters $a = 6.5971(2)$ Å, $b = 9.8791(3)$ Å and $c = 10.8819(3)$ Å in the $K_2ZnSi_2O_6$ structure type. The crystal structure consists of a three-dimensional network, composed of Co and mixed Co/Ge tetrahedra, and features cavities occupied by Rb cations.

Graphic Abstract

X-ray diffraction quality single crystals of a novel rubidium cobalt germanate, $Rb_2Co_{1.85}Ge_{1.15}O_6$, were grown by soaking a pre-reacted powder, targeted for preparing $Rb_{4.51}Co_{2.35}Ge_{5.10}O_{15}F_{1.96}$, in a RbCl-RbF eutectic melt at 700 °C. The complex was characterized by single crystal X-ray diffraction and found to crystallize in the orthorhombic space group $C222_1$ in the $K_2ZnSi_2O_6$ structure type.

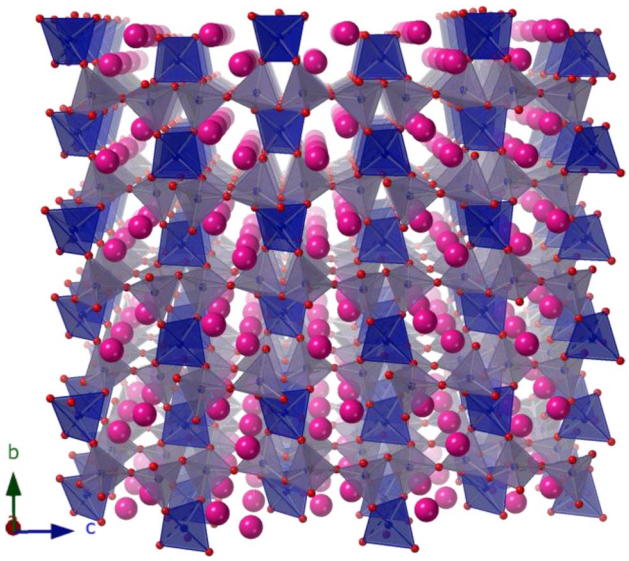

Keywords Noncentrosymmetric · Crystal growth · Cobalt germanate

Electronic supplementary material The online version of this article (https://doi.org/10.1007/s10870-020-00868-9) contains supplementary material, which is available to authorized users.

Extended author information available on the last page of the article

Published online: 24 October 2020

Introduction

Quaternary alkali cobalt germanates are exceedingly rare. A quick ICSD database search reveals that $Li_2CoGe_3O_8$ and Na_2CoGeO_4 are the only two complex quaternary cobalt oxides that have been characterized as high quality single crystals [1, 2]. To the best of our knowledge, no reports exist on K or Rb containing cobalt germanates characterized via single crystal X-ray diffraction. One possible reason for the dearth of reports on the crystal structures of cobalt germanates, as well as silicates, could be the extreme complexity exhibited by their crystal structures, which is caused by Co/*T* (*T* = Si, Ge) site mixing. This was empirically observed in our recent report on complex cesium containing cobalt silicates and germanates, all of which exhibit site mixing [3]. In addition to the need for further exploration of the *A*/Co/Ge/O (*A* = alkali metal) phase space, interest in this group of materials arises from their frequent crystallization in noncentrosymmetric structure types, thereby, rendering these materials attractive candidates for applications in non-linear optics [4, 5]. Another reason for exploring the *A*/*M*/Ge/O (*A* = alkali metal; *M* = transition metal) phase space is to take advantage of the propensity of these materials to crystallize in a wide variety of complex three-dimensional structure types that often contain channels occupied by alkali metal cations for charge balance. These structure types include pollucites, leucites, pyroxenes as well as several new structure types, some of which we previously reported for a few complex cobalt silicates and germanates [3, 6–8]. The presence of large cavities or channels in these structures coupled with their rigid anionic frameworks, makes them potential materials for ion-exchange applications in hot, aqueous salt solutions as well as molten alkali nitrate salt baths. Furthermore, the application of the molten salt flux crystal growth approach enables the formation of these systems as single crystalline polymorphs with closely related structures, but strikingly different properties [9].

Herein, we report on the synthesis and crystal structure of the first quaternary rubidium cobalt germanate, $Rb_2Co_{1.85}Ge_{1.15}O_6$, grown as single crystals by soaking a pre-reacted polycrystalline powder in molten RbCl-RbF eutectic flux.

Experimental

Synthesis

Co_3O_4 (Matheson Coleman & Bell), GeO_2 (99.999%, Alfa Aesar), RbCl (99.8%, Alfa Aesar) and RbF (99.1%, Alfa Aesar) were used as received without further modification for the synthesis $Rb_2Co_{1.85}Ge_{1.15}O_6$.

The solid-state synthesis for the preparation of $Rb_{4.51}Co_{2.35}Ge_{5.10}O_{15}F_{1.96}$ was attempted by mixing stoichiometric amounts of RbF, Rb_2CO_3, Co_3O_4 and GeO_2, and firing them at 700 °C for 24 h in an alumina crucible. Powder X-ray diffraction (PXRD) data collection on the resultant polycrystalline powder indicated it to be an unknown phase and showed no evidence of the targeted $Rb_{4.51}Co_{2.35}Ge_{5.10}O_{15}F_{1.96}$ phase (Figure S1). For structural characterization, the unknown phase was crystallized by layering 0.2 g of it beneath a mixture of 1.34 g of RbCl and 1.02 g of RbF in a 7.5 cm tall by 1.2 cm diameter cylindrical silver crucible with one of its ends sealed and welded shut. After crimping the other end of the crucible shut, it was placed into a programmable furnace. The tube containing the charge was heated at 10 °C/min to 700 °C, maintained at this temperature for 12 h, slow cooled at 6 °C/h to 500 °C, and then fast cooled to room temperature by shutting the furnace off. Once cooled to ambient temperature, the solidified RbCl-RbF flux was dissolved in distilled hot water, aided by sonication, and the resulting deep blue, prism-shaped crystals were isolated via vacuum filtration in approximately 20% yield. The average size of the crystals was approximately $0.12 \times 0.08 \times 0.05$ mm^3. The final composition of the resulting crystals was established using single crystal X-ray diffraction.

Powder X-ray Diffraction (PXRD)

Powder X-ray diffraction data were collected on a Bruker D2 Phaser using Cu Kα radiation ($\lambda = 1.54018$ Å) and equipped with a LYNXEYE silicon strip detector. The scan covered the angular range 10–70° in steps of 0.02°.

Energy Dispersive Spectroscopy (EDS)

EDS was performed on a deep blue prism using a TESCAN Vega-3 SBU scanning electron microscope (SEM) with a Thermo EDS attachment operated in an ultralow vacuum mode. The crystal was mounted on an SEM stub with carbon tape and analyzed using 20 kV accelerating voltage and an accumulation time of 20 s. EDS verified the presence of Rb, Co, Ge and O. Fig. S2 illustrates the EDS spectrum and SEM image for $Rb_2Co_{1.85}Ge_{1.15}O_6$.

Single Crystal X-ray Diffraction (SCXRD)

X-ray intensity data from a deep blue prism were collected at 301(2) K using a Bruker D8 QUEST diffractometer equipped with a PHOTON 100 CMOS area detector and an Incoatec microfocus source (Mo Kα radiation, $\lambda = 0.71073$ Å) [10]. The data collection covered 99.9% of reciprocal space to

$2\theta_{max} = 75.64°$, with an average reflection redundancy of 17.5 and $R_{int} = 0.028$ after absorption correction. The raw area detector data frames were reduced, scaled and corrected for absorption effects using the SAINT + and SADABS programs [10, 11]. Final unit cell parameters were determined by least-squares refinement of 9924 reflections taken from the data set. An initial structural model was obtained with SHELXT [12]. Subsequent difference Fourier calculations and full-matrix least-squares refinement against F^2 were performed with SHELXL-2018 using the ShelXle interface [13, 14].

The compound crystallizes in the orthorhombic system. The space group $C222_1$ was uniquely determined by the pattern of systematic absences in the intensity data and was confirmed by structure solution. The asymmetric unit consists of one rubidium atom, one mixed Ge/Co site, one pure Co site and four unique oxygen atoms. Rb(1), the mixed Ge/Co site and oxygen atoms O(1) and O(2) are all located on positions of general crystallographic symmetry (site 8*c*). The pure cobalt site Co(1) and oxygen O(3) are located on two-fold axes of rotation (site 4*b*, 0.2. site symmetry). Oxygen O(4) is located on the two-fold axis of site 4*a* (site symmetry 2..). Initially a model with all sites fully occupied was refined, giving $R_1/wR_2 = 0.019/0.060$ and $\Delta\rho(\text{max/min}) = +0.94/-1.25 e^-/Å^3$. The deepest hole is located at the Ge(1) site. Trial refinements of the metal atom site occupation factors (*sof*s) showed a significant deviation from full occupancy only for the Ge(1) site. The Rb(1) and Co(1) sites, and also all oxygen sites, refined to 100% occupancy within experimental error. *sof*(Ge1) refined to 0.910(1), and was accompanied by a decrease in *R*-values from $R_1/wR_2 = 0.019/0.060$ to 0.011/0.028. The difference map also improved to $+0.38/-0.41 e^-/Å^3$. The combined observation of the significantly lower residuals and difference map flattening gives strong support for a scattering deficiency on the 8*c* Ge(1) site. This could be interpreted as: (1) Ge vacancy or (2) admixture of cobalt onto the Ge1 site. Refinement of a mixed site Ge(1)/Co(1A), with the total site occupancy constrained to one, yielded *sof*(Ge1/Co1A) = 0.577(7)/0.423(7). A model with simultaneous Co/Ge mixing and vacancies is also possible but cannot be defined. Trial refinements of both models (1) and (2) gave similar refinement statistics ($R_1/wR_2 = 0.011/0.028$; for the vacancy model and 0.011/0.027 for the Co/Ge mixing model) and cannot be reliably distinguished from the X-ray data. The crystal composition derived from each model is: (1) vacancy: $Rb_2CoGe_{1.83}O_6$, (2) Ge/Co mixing: $Rb_2Co_{1.85(1)}Ge_{1.15(1)}O_6$. The two models generate average cobalt oxidation states of (1), + 2.68 (2) + 2.92. Since the average oxidation state of model (2) is closer to that in the starting material Co_2O_3, and because a tetrahedral Ge vacancy model is less likely than site mixing, model (2) is reported here. Cobalt mixing onto the Ge(1) site implies short Co–O distances of 1.71–1.78 Å, compared to the more normal Co–O distances of 1.95–1.98 Å at the Co(1) site. This could be explained by positional uncertainty of the oxygen sites, i.e. 42.3% of the oxygen sites around Ge(1)/Co(1) are located slightly further away from the metal center than the reported positions but are too closely overlapped for a stable refinement of a two-site model. The slight displacement is absorbed by the anisotropic displacement parameters and cannot be positionally resolved. All atoms were refined with anisotropic displacement parameters. The largest residual electron density peak and hole in the final difference map are + 0.37 and − 0.44 $e^-/Å^3$, located 1.49 Å from Rb(1) and 0.64 Å from Ge(1)/Co(1A). The absolute structure (Flack) parameter after the final refinement cycles was − 0.002(3).

Fluorine: during the structure solution the direct refinement of the occupancies for the O sites gave 100% oxygen, with no evidence for a heavier atom on the site. With such good data (R1 = 1% with a high-resolution dataset and a small and flat residual difference map), O and F can in fact be reliably distinguished. It is always possible that a very small concentration of F exists somewhere, mixed with O, but it would not be detectable by X-ray diffraction means. For that reason, the composition is best described as a pure oxide.

Results and Discussion

Synthesis

Mixed-alkali fluoride-chloride melts work very well for crystallizing a wide array of complex germanates [15–17]. Compared to a single component flux, mixed fluxes have lower melting points, and the fluoride precursor provides the added advantage of acting as a mineralizer. A mixed RbCl–RbF flux was, therefore, considered to be the best flux for exploring the crystallization of Rb–Co–Ge–O phases, such as the title compound $Rb_2Co_{1.85}Ge_{1.15}O_6$. It is interesting to note that $Rb_2Co_{1.85}Ge_{1.15}O_6$ cannot be prepared using a conventional solid state synthesis approach. A number of attempts were made to synthesize $Rb_2Co_{1.85}Ge_{1.15}O_6$ using Rb_2CO_3 or $RbNO_3$, and elemental Ge or GeO_2, as Rb and Ge sources, respectively; all, however, resulted in either a viscous or a hardened, dark blue matrix that was extremely difficult to remove from the alumina crucible upon completion of the reaction. Soaking a pre-reacted powder intended to synthesize $Rb_{4.51}Co_{2.35}Ge_{5.10}O_{15}F_{1.96}$ in a RbCl-RbF eutectic melt has proven to be the only viable route to crystallize $Rb_2Co_{1.85}Ge_{1.15}O_6$, thus far. Treating $Rb_2Co_{1.85}Ge_{1.15}O_6$ single crystals in a molten KNO_3 bath at 350 ºC in order to exchange Rb for K did not lead to the desired ion exchange.

Crystal Structure

$Rb_2Co_{1.85}Ge_{1.15}O_6$ crystallizes in the orthorhombic system in the polar, noncentrosymmetric space group $C222_1$ in the $K_2ZnSi_2O_6$ structure type [18]. The asymmetric unit consists of one Rb atom, one pure Co site, one mixed Ge/Co site modeled as 58/42 Ge/Co, and four oxygen atoms. It is worth noticing that the known $K_2ZnT_2O_6$ (T = Si, Ge) structure exhibits no site disorder and its crystal structure only features pure *T* and Zn sites. Crystallographic and refinement data for $Rb_2Co_{1.85}Ge_{1.15}O_6$ can be found in Table 1. Atomic coordinates are listed in Table 2 and selected interatomic distances are provided in Table 3. The crystal structure of the complex is composed of chains built from corner sharing $(Ge/Co)O_4$ tetrahedra running down the *c*-axis. As shown in Fig. 1, each chain is made from $(Ge/Co)O_4$ dimers that alternate in facing-up (UU) and facing-down (DD) fashion. Each pair of monomers is connected via O(4), while each dimer (UU) is bridged to the other (DD) via O(3). The bond lengths in $(Ge/Co)O_4$ tetrahedra range from 1.7053(13)–1.7776(10) Å, which are in agreement with those reported elsewhere [3]. The $(Ge/Co)O_4$ zigzag chains are linked via isolated CoO_4 tetrahedra to produce a three-dimensional, $[Co_2GeO_6]^{2-}$ framework that contains channels crisscrossing the structure in all three dimensions. The CoO_4 tetrahedra consist of a Co(1) atom bonded to two O(1) atoms and two O(2) atoms with bond lengths 1.9509(12) Å and 1.9821(13) Å, respectively. The channels formed by the three-dimensional assembly of CoO_4 and $(Ge/Co)O_4$ tetrahedra are filled by Rb^+ cations that provide charge balance to the structure. An overall polyhedral representation for the $Rb_2Co_{1.85}Ge_{1.15}O_6$ crystal structure is provided in Fig. 2.

It is worth noticing that the 1:1:2:6 AMT_2O_6 and 2:1:2:6 $A_2MT_2O_6$ (A = alkali metal; M = transition metal; and T = Si, Ge) compositions crystallize in distinctly different three dimensional structure types. For example, $CsFeSi_2O_6$ crystallizes in the centrosymmetric, cubic space group *Ia*-3d in the well-known pollucite structure type that is found for a variety of zeolite minerals with the general formula $(Cs, Na)_2Al_2Si_4O_{12}{\cdot}2H_2O$ with Fe, Ca, Rb and K as common substituting elements [6]. As the alkali metal size reduces upon moving up from Cs to Rb or K, in $AFeSi_2O_6$, the structure type changes to leucite-low; however, the space group remains unchanged [7]. As the counter cation size in the $AFeSi_2O_6$ structure further shrinks upon switching to Na, the crystal setting is lowered to monoclinic symmetry in space group *C*2/*c* in the pyroxene or $CaMgSi_2O_6$ structure type [8].

In contrast to the widely known and ubiquitous 1:1:2:6 AMT_2O_6 systems, the 2:1:2:6 $A_2MT_2O_6$ compositions are rather scarce and exhibit structure types featuring three-dimensional frameworks that are quite different from those exhibited by AMT_2O_6 systems (Fig. 3). For instance, $K_2ZnT_2O_6$ (*T* = Si, Ge) crystallize in a new structure type in the polar, noncentrosymmetric space group $C222_1$ [18, 19]. $Rb_2Co_{1.85}Ge_{1.15}O_6$, the compound reported herein, crystallizes in the same structure type as $K_2ZnT_2O_6$ (*T* = Si, Ge). It is important to emphasize how the 1:1:2:6 AMT_2O_6 and 2:1:2:6 $A_2MT_2O_6$ compositions,

Table 1 Crystallographic and refinement data for $Rb_2Co_{1.85}Ge_{1.15}O_6$

Chemical formula	$Rb_2Co_{1.85}Ge_{1.15}O_6$
Crystal color and habit	Deep blue prism
Formula weight (g mol^{-1})	459.49
Temperature (K)	301(2)
Space group	$C222_1$
a (Å)	6.5971(2)
b (Å)	9.8791(3)
c (Å)	10.8819(3)
V ($Å^3$)	709.21(4)
Z	4
Density (Mg m^{-3})	4.303
Crystal size (mm × mm × mm)	0.140 × 0.080 × 0.060
θ_{max} (°)	37.822
Reflections collected	1912
Goodness-of-fit on F^2	1.107
Flack parameter	−0.002(3)
R indices	$R_1 = 0.0109$; $wR_2 = 0.0268$
Largest diff. peak and hole (e^- and $Å^{-3}$)	0.367 and -0.436

Table 2 Atomic coordinates (× 10^4) and equivalent isotropic displacement parameters ($Å^2 \times 10^3$) for $Rb_2Co_{1.85}Ge_{1.15}O_6$. U(eq) is defined as one third of the trace of the orthogonalized U^{ij} tensor

Atom	Occupancy	*x*	*y*	*z*	Ueq [$Å^2$]
Rb(1)		1123(1)	1734(1)	754(1)	25(1)
Ge(1)	0.577(7)	1536(1)	5176(1)	1388(1)	13(1)
Co(1A)	0.423(7)	1536(1)	5176(1)	1388(1)	13(1)
Co(1)		5000	3102(1)	2500	14(1)
O(1)		3688(2)	4219(1)	1254(1)	19(1)
O(2)		1930(2)	6849(1)	1691(1)	20(1)
O(3)		0	4411(2)	2500	24(1)
O(4)		140(3)	5000	0	20(1)

Table 3 Select interatomic distances (Å) of cation coordination spheres in $Rb_2Co_{1.85}Ge_{1.15}O_6$

Bond	Distance
Ge/Co(1) –O(1)	1.7119(13)
Ge/Co(1) –O(2)	1.7053(13)
Ge/Co(1) –O(3)	1.7501(8)
Ge/Co(1) –O(4)	1.7776(10)
Co(1)–O(1) (×2)	1.9509(12)
Co(1)–O(2) (×2)	1.9821(13)

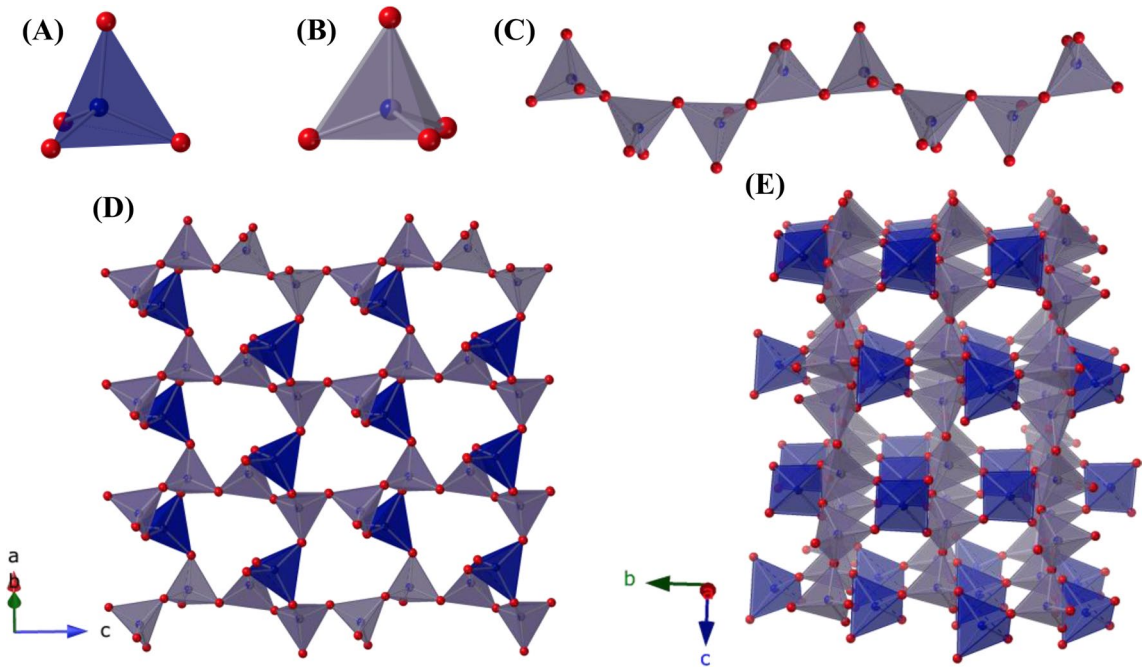

Fig. 1 **a** CoO_4 unit and **b** $(Ge/Co)O_4$ unit corner-sharing to form **c** $(Ge/Co)O_4$ chains which are connected together via CoO_4 tetrahedra to form a three-dimensional $[Co_2GeO_6]^{2-}$ anionic framework shown in **e** down the *a*-axis. A single $[Co_2GeO_6]^{2-}$ layer formed through corner-shared CoO_4 and $(Ge/Co)O_4$ tetrahedra is shown in **d**. Co atoms, mixed Ge/Co sites, and O are represented in lavender, deep blue, and red, respectively

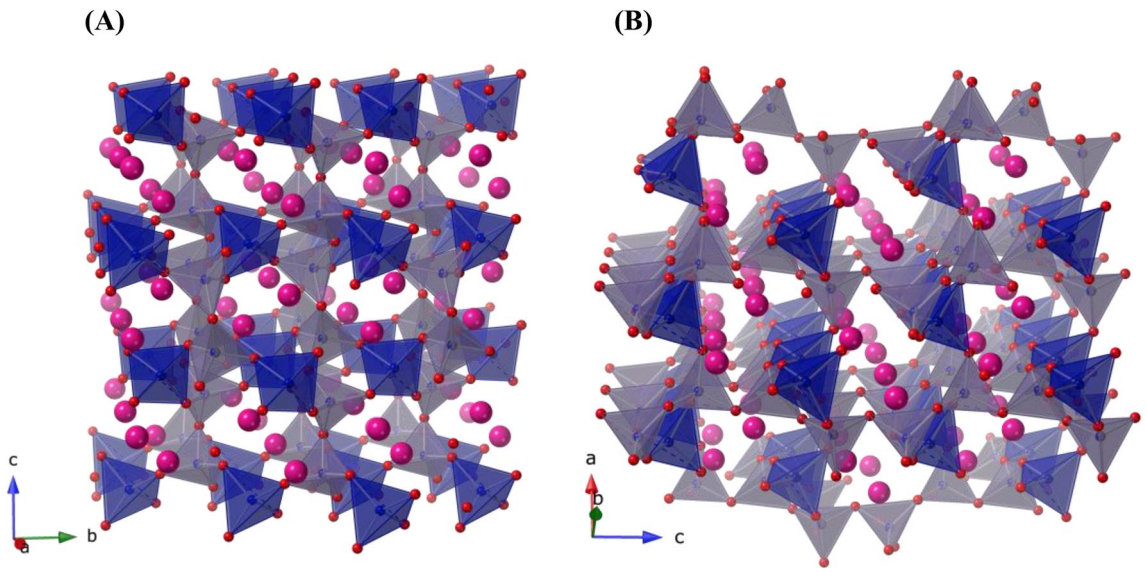

Fig. 2 Perspective views of the $Rb_2Co_{1.85}Ge_{1.15}O_6$crystal structure down the *a*-axis and *b*-axis shown in **a**, **b**, respectively

so far, have been observed to crystallize in centrosymmetric and noncentrosymmetric space groups, respectively. Future endeavors will be aimed at replacing Rb, in $Rb_2Co_{1.85}Ge_{1.15}O_6$, with smaller alkali metals such as Na or K, and Cs, in order to study the effect of alkali size

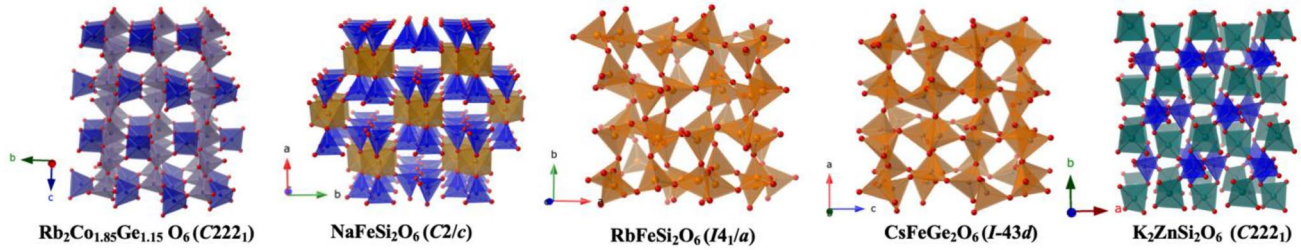

Fig. 3 Illustration of different frameworks exhibited by the 2:2:1:6, 1:1:2:6, and 2:1:2:6 silicates and germanates. Fe in $NaFeSi_2O_6$ is six-coordinated. $RbFeSi_2O_6$ and $CsFeGe_2O_6$ exhibit mixed Fe/T (T = Si, Ge) sites. $Rb_2Co_{1.85}Ge_{1.15}O_6$ features, both, unique Co and mixed Co/Ge sites. $K_2ZnSi_2O_6$ exhibits unique Zn and Si sites, shown in teal and blue, respectively

on the crystal symmetry of $A_2Co_2GeO_6$, and compare and contrast its structural features with AMT_2O_6 systems.

Conclusion

A novel quaternary, noncentrosymmetric rubidium cobalt germanate, $Rb_2Co_{1.85}Ge_{1.15}O_6$, was synthesized via molten salt flux growth approach and its structure determined via single crystal X-ray diffraction. Future experiments will focus on crystallizing other members of the series containing different alkali metals and performing their physical property measurements.

Acknowledgements The authors gratefully acknowledge the U.S. National Science Foundation through Award OIA-1655740.

References

1. Kawai H, Tabuchi M, Nagata M, Tukamoto H, West AR (1998) J Mater Chem 8:1273–1280
2. Maksimov BA, Ilyukhin VV, Belov NV (1978) Dokl Akad Nauk SSSR 242:1070–1073
3. Usman M, Smith MD, Kocevski V, Besmann T, zur Loye HC (2020) CrystEngComm 22:1112–1119
4. Halasyamani PS, Poeppelmeier KR (1998) Chem Mater 10(10):2753–2769
5. Usman M, Smith MD, Morrison G, Klepov VV, Zhang W, Halasyamani PS, zur Loye HC (2019) Inorg Chem 58(13):8541–8550
6. Kopp OC, Harris LA, Clark GW, Yakel HL Jr (1963) Am Miner 48:100–109
7. Bell AMT, Henderson CMB (1994) Acta Cryst C 50:1531–1536
8. Clark JR, Appleman DE, Papike JJ (1969) Miner Soc Am 2:31–50
9. Usman M, Kocevski V, Smith MD, Morrison G, Zhang W, Besmann T, Halasyamani PS, zur Loye HC (2020). Inorg Chem. https://doi.org/10.1021/acs.inorgchem.0c00936
10. AXS Bruker (2016) APEX3 version 2016.5-0 and SAINT+ version 8.37A. Bruker AXS Inc., Madison
11. Krause L, Herbst Irmer R, Sheldrick GM, Stalke D (2015) J Appl Cryst 48:3–10
12. Sheldrick GM (2015a) Acta Cryst A 71:3–8
13. Sheldrick GM (2015b) Acta Cryst C 71:3–8
14. Hübschle CB, Sheldrick GM, Bittrich B (2011) J Appl Cryst 44:1281–1284
15. Spagnuolo NR, Morrison G, Zur Loye HC (2019) Solid State Sci 97:105973
16. Morrison G, Kocevski V, Misture ST, Spagnuolo NR, Hines AT, Besmann T, zur Loye HC (2019) Inorg Chem 19(10):5477–5482
17. Li H, Kegler P, Alekseev EV (2020) Dalton Trans 49:2244–2257
18. Hogrefe AR, Czank M (1995) Acta Cryst C51:1728–1730
19. Grins J, Werner PE (1989) Acta Chem Scand 43:11–14

Publisher's Note Springer Nature remains neutral with regard to jurisdictional claims in published maps and institutional affiliations.

Affiliations

Mohammad Usman[1] · Mark D. Smith[1] · Hans-Conrad zur Loye[1]

✉ Hans-Conrad zur Loye
zurloye@mailbox.sc.edu

[1] Department of Chemistry and Biochemistry, University of South Carolina, Columbia, SC 29208, USA